Bulletin of Volcanology (2025) 87:110
https://doi.org/10.1007/s00445-025-01899-w

RESEARCH ARTICLE

The influence of grain size and channelization on mobility of volcanic granular flows: insights from laboratory experiments

Roberto Sulpizio[1,2,3] · Sara Meschiari[4] · Damiano Sarocchi[5,6] · Francesco Neglia[1] · Luis Angel Rodriguez-Sedano[5] · Federico Lucchi[4] · Oscar Segura-Cisneros[5] · Fabio Dioguardi[1] · Bernardino Barrientos[7]

Received: 6 March 2025 / Accepted: 13 October 2025 / Published online: 8 November 2025

Abstract

Laboratory experiments on granular flows using natural material were carried out under different conditions in order to investigate the behavior of fine to coarse-grained, channelized and non-channelized granular flows passing over a break in slope. Morphometric parameters of channelized and non-channelized experiments are compared for both fine-grained and coarse-grained grain size distributions. After normalization, morphometric data provide empirical relationships that highlight the major influence of grain size vs. channelization of the experimental flows. Normalized velocity data of the flow front show third-order polynomial fit for both coarse-grained and fine-grained experiments, as well as for non-channelized and channelized ones. This highlights similar complex behavior of the different experimental flows, which differs only for different partition of inertial and frictional forces at changing grain size of experimental mixtures. The runout of coarse-grained granular flows is always longer than that of fine-grained granular flows, irrespective if they are channelized or non-channelized. Finally, we discuss the applicability of the experimental results to natural granular flows, highlighting the change in physical behavior of fine-rich pyroclastic density currents and volcaniclastic flows depending on the effectiveness of fluidization processes in fine-grained natural materials.

Keywords Granular flows · Experiments · Pyroclastic density currents · Volcaniclastic flows

Editorial responsibility: O. Roche

✉ Roberto Sulpizio
roberto.sulpizio@uniba.it

[1] Dipartimento Di Scienze Della Terra E Geoambientali, University of Bari "Aldo Moro", Via Orabona 4, 70125 Bari, Italy

[2] IGAG-CNR, Via M. Bianco 9, Milan, Italy

[3] INGV Section of Bologna, Viale Carlo Berti Pichat, 6/2, Bologna, Italy

[4] Dipartimento Di Scienze Biologiche, Geologiche ed Ambientali, Piazza Di Porta San Donato, 1, 40126 Bologna, Italy

[5] Instituto de Geología, Universidad Autónoma de San Luis Potosí, Dr. M. Nava No. 5, Zona Universitaria, San Luis Potosí 78240, México

[6] CONACYT-Instituto de Geología, Universidad Autónoma de San Luis Potosí, Zona Universitaria, Av. Dr. M. Nava No 5, 78240 San Luis Potosí, México

[7] Centro de Investigaciones en Óptica, A. C., Loma del Bosque 115, 37150 León, Gto, Mexico

Introduction

Many hazardous natural processes, like snow avalanches, landslides, debris flows and pyroclastic density currents (PDCs) are dominated by granular flow processes (Iverson 1997; Branney and Kokelaar 2002; Zanchetta et al. 2004; Louge et al. 2012; Sulpizio et al. 2014; Jones et al. 2023), being characterized by complex interactions between solid grains and an interstitial fluid phase that ultimately control their motion, deposition and final runout (Campbell 2006; Iverson and Vallance 2001). In volcanic settings, the physics of granular flows particularly controls the dynamics of concentrated PDCs and debris flows, which are among the most dangerous phenomena related to volcanic activity, threatening life and producing great economic loss around the world (Tilling and Lipman 1993; Tanguy et al. 1998; Gurioli et al. 2010). The mobility of natural volcanic granular flows (e.g. concentrated pyroclastic density currents, debris flows) is a major topic in volcanology (Hayashi and Self 1992; Dade and Huppert 1998; Calder et al. 2000; Breard et al. 2018; Palladino and Giordano 2019), but it has relevance also for

snow avalanches (Vallet et al. 2004; Turnbull et al. 2007; Louge et al. 2012) and granular flow studies (e.g. Gray et al. 1999; Pudasaini and Hutter 2007; Pudasaini 2012).

The dynamics of (dry) granular flows, in terms of particle segregation, erosion and rate of deposition, is directly influenced by local variations of the topographic slopes, as documented in volcanic areas and other sedimentary settings (e.g. Macias et al. 1998; Calder et al. 2000; Denlinger and Iverson 2001; Mulder and Alexander 2001; Felix and Thomas 2004; Zanchetta et al. 2004; Cole et al. 2005; Gray et al. 2005; Lube et al. 2007; 2011; Sulpizio et al. 2007; 2010; Bernard et al. 2014). However, accurate physical models describing the motion of granular flows over topography are few and not exhaustive (Gray et al. 1999; Denlinger and Iverson 2001; Iverson et al. 2004), due to the complex feedbacks between moving particulate matter and real topography at a millimeter to decameter scale, although recent advances from laboratory experiments shed new light on the influence of the slope on flow overspilling at channel bends in channelized granular flows. This implies that the effects of grain size distribution of the granular flow and length of confinement within valleys and channels are largely undetermined, as well as their influence on flow dynamics and runout.

The motion of natural volcanic granular flows is difficult to observe, because of their very hostile nature, while the collection of geological data from past deposits is very extensive but non-decisive for reconstructions of the behavior of the corresponding avalanches. It descends that laboratory experiments, although affected by scaling issues sometimes difficult to overcome (e.g., Iverson 2015), are usually the best compromise between analysis of deposits and direct observation of parent flows at natural scale. Here, we present the results of a number of laboratory experiments that simulate the behavior of granular flows engineered and carried out using a 5-m-long flume (Fig. 1a) and natural volcanic particles. The experiments deal with the runouts of both channelized and unconfined flows using coarse or fine-grained volcanic material moving across a break in slope. In particular, the results of coarse-grained granular flows in unconfined conditions provided by Sulpizio et al. (2016) are here complemented and compared with experiments carried out using fine-grained material and a channelized version of the coarse-grained flows previously studied by Sulpizio et al. (2016). The results highlight some significant feedbacks on flow mobility among slope changes, grain size and flow channelization, which may provide important insights for the comprehension of natural granular flows.

Experimental setup

The laboratory experiments were carried out using a flume facility, designed and built at the Instituto de Geología of Universidad Autónoma de San Luis Potosí (Mexico), using a plastic rough-bottom with transparent glass sidewalls, which allow real-time observation of the moving granular avalanches (see Sulpizio et al. 2016 for details). It is a modular apparatus, whose geometric characteristics can be modified to arrange different experimental setups. The facility consists of the following sections (Fig. 1a): (1) a charge system, consisting of a container of 0.036 m^3 (hopper) with a remotely controlled electromagnetic opening system releasing the granular material from 0.4 m height above the flume; (2) a 5.0 m long and 0.3 wide channel with constant slope

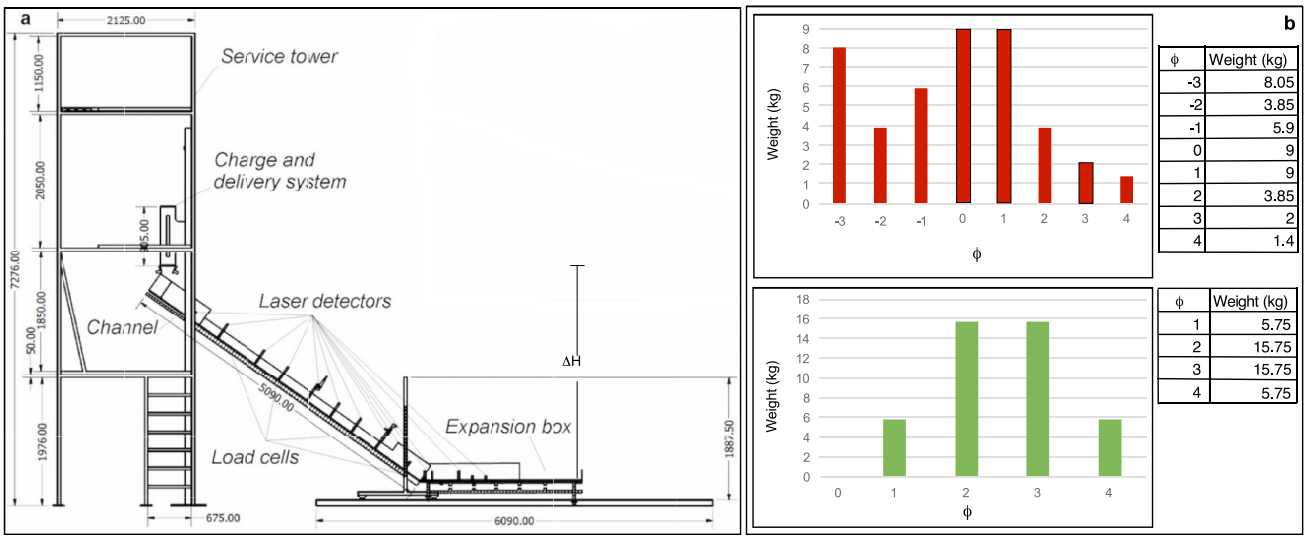

Fig. 1 Design of the experimental flume. (**a**) Sketch of the charge and delivery system, flume and expansion box. (**b**) Grain size histograms and tables for material used for coarse-grained and fine-grained experiments

angle (which can be changed by the operator); and (3) an expansion area, with inclination that can vary between 0° and 20°, where the granular material decelerates and deposits. We run two different types of experiments where the deceleration of the granular flows occurred in (i) confined and (ii) unconfined conditions. In the first case, the channel was prolonged within the expansion area using glass walls that delimited a channel of the same width, while in the second case the granular material was left to expand unconfined in the expansion area (Sulpizio et al. 2016). In the first set of experiments (see also Sulpizio et al. 2016), we monitored the flows with three medium-speed (60 fps) high-resolution (1920 × 1080 pixel) camcorders (SONY HDR-CX240) and a GoPro (Hero3 model) with wide-angle zenithal vision. In the second set of experiments (with channelized deposition area), three Nikon1 J1 cameras (400 fps and 640 × 240-pixel resolution) were used, as well as a GoPro hero 7 camera for a zenithal panoramic view. Both experiments were monitored by means of 14 laser barriers, detecting the flow front velocities and allowing the characterization of the flow kinematic (Fig. 1a).

The experimental runs were performed with a (constant) channel inclination of 40°, whereas the inclination of the expansion box varied between 0° and 20°, at 5° increments. We define the slope-angle ratio (SR) as the ratio between the slope angle in the expansion box (depositional area) and that in the upstream channel (charge area), so that lower SRs indicate greater breaks in slope. Three experiments for each SR were carried out. We used 43 kg of granular material, represented by moderately vesicular, dacitic pyroclastics (density ca. 2300 kg m^{-3}) from the Nevado de Toluca volcano (Mexico), of two different grainsize distributions as displayed in Fig. 1b: coarse-grained (30° internal and 35° basal friction angle of material) and fine-grained (32° internal and 37° basal friction angle of material). Specifically, in order to obtain the two distributions, the material was first sieved at 1φ interval ($\varphi = -\log_2 d$, where d is the particle diameter in mm). The sieved material was then assembled in order to obtain a coarse-grained Weibull distribution, modified with the addition of coarse-grained material (−3φ; 8 mm), and a fine-grained Gaussian distribution (Fig. 1b). The internal friction angle was determined by measuring the slope of a conical pile formed by the material on a horizontal surface. The basal friction angle was assessed by gradually increasing the inclination of a plane covered with the same plastic material used for the base of the experimental channel and expansion box, and it was assumed to be equal to the critical slope angle at which basal sliding of the material was first observed.

The roughness of the plastic material was calculated using a Profilometer MAHR, model MarSurf PCV 200 GD 25 (precision of 30 nm), measured on longitudinal section of 25 mm. The measured roughness parameters are *Ra* (mean arithmetic roughness), *Rq* (quadratic mean roughness), and *Rz* (mean peak-to-valley height), in agreement with ISO 4287/1 and DIN 4768 international standards for surface texture and roughness measurement. The roughness parameters are reported in Table 1.

Results

We describe here the original results of the experiments carried out using fine-grained material in confined and unconfined conditions and using channelized coarse-grained material, which are compared with those of coarse-grained unconfined granular flows described by Sulpizio et al. (2016).

In these previous experiments, the focus was on the effect of changing break in slope on runout of a granular flow with a Weibull-modified grain size distribution spreading unconfined on the expansion area. In the new experiments described in this paper, we used the same Weibull-modified grain size distribution for analyzing runout of channelized granular flows, and fine-grained Gaussian grain size distribution for both channelized and non-channelized flows. The material charged in the hopper hits the flume base after 0.40 m of free fall. Following the impact with the flume bottom, the material accelerates until the break in slope, beyond the granular flow starts to spread unconfined (then decelerating) in the expansion box (Fig. 2a) or decelerates confined in the channel (Fig. 2b, c). The unconfined flow deposits show elliptical shapes (Fig. 2a), similar to those observed for coarse-grained granular flow experiments (Sulpizio et al. 2016).

The results of experiments using two different grain size distributions in channelized or non-channelized conditions highlight similar behaviors in terms of the relationships between runout and SR. Here we define the normalized runout as the ratio between the distance travelled beyond the break in slope for each experiment (D), which is the effective runout of the flows, and the difference in height between the hopper gate and the deposit in the expansion box (ΔH) (Fig. 1a). Non-channelized experiments show a linear dependence of the normalized runout on SR for

Table 1 Roughness parameters for the plastic substrate used in the experiments. The measurements were carried out on three longitudinal windows of 25 mm in length. *Ra* = mean arithmetic roughness; *Rq* = quadratic mean roughness; *Rz* = mean peak-to-valley height

Roughness parameter	Measurement 1	Measurement 2	Measurement 3
Ra (μm)	12.0703	12.1897	12.2337
Rq (μm)	16.1916	16.3047	16.3667
Rz (μm)	72.3577	72.3904	72.4681

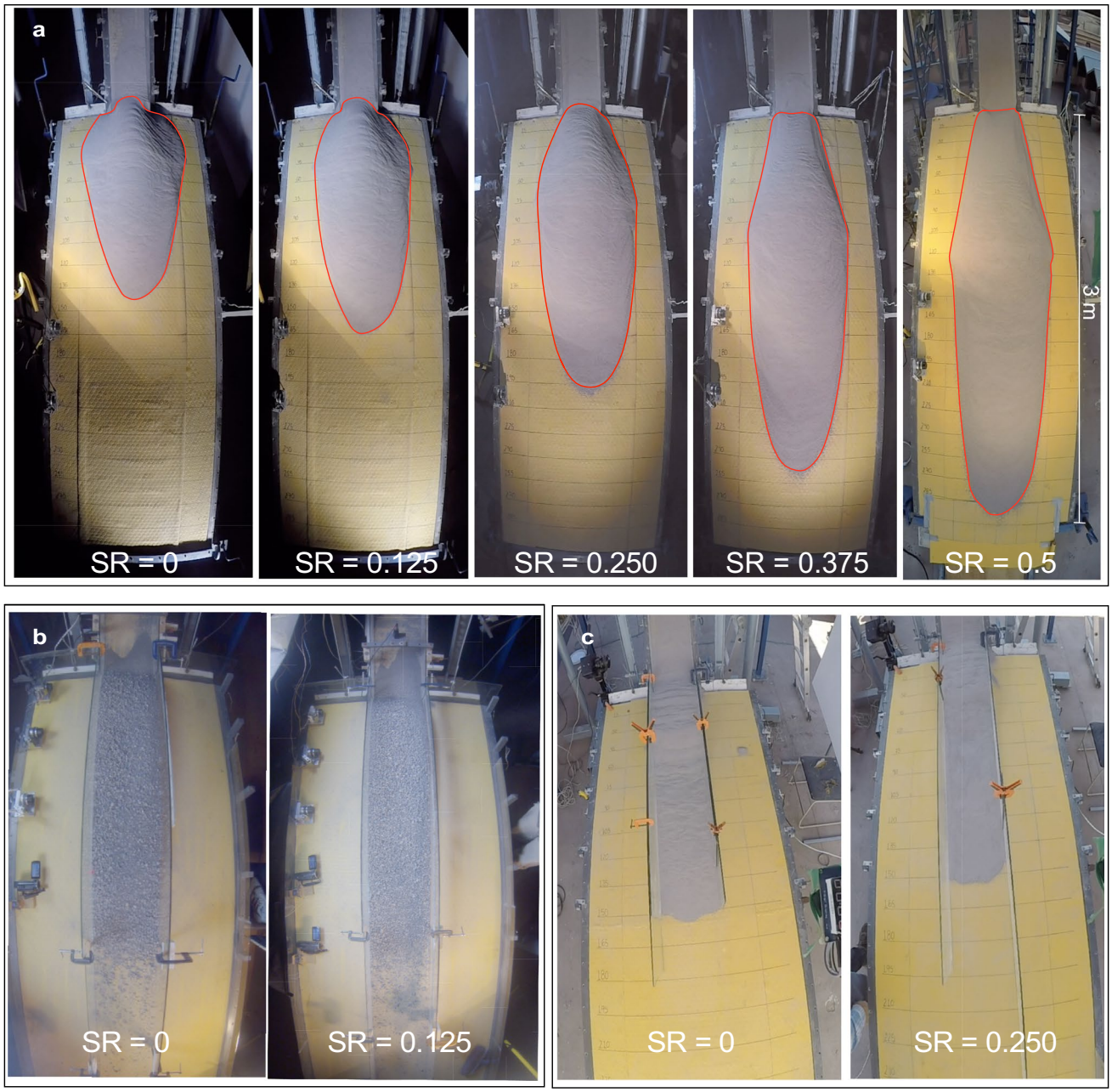

Fig. 2 View of non-channelized and channelized deposits using different slope ratio (SR) values. (**a**) Deposits of fine-grained experiments. The red contours were used for calculation of morphological parameters; (**b**) examples of channelized deposits for coarse-grained (two pictures on the left) and fine-grained (two pictures on the right) experiments

experiments carried out with both coarse-grained and fine-grained material (Fig. 3a). The runouts are similar for low SR values (0 to 0.125), but they diverge at increasing SR values (Fig. 3a). This is clearly expressed by the different slopes of the two regression lines, passing from 1.1 for the fine-grained grain size to 1.5 for the coarse-grained one. Channelized experiments show a behavior very similar to non-channelized ones, with slopes that vary from 1.2 for fine-grained material to 1.6 for coarse-grained one (Fig. 3b). The comparison of experiments using the same grain size in channelized and non-channelized conditions shows quite similar regression lines, with only a limited increase shift of 5–10% in favor of channelized experiments (Fig. 3c, d).

To investigate the depositional behavior in the different experimental conditions, we plotted also the position of the maximum thickness relative to SR (Fig. 4). The position of the maximum thickness is expressed as the ratio between the distance at which the maximum thickness of the deposits is

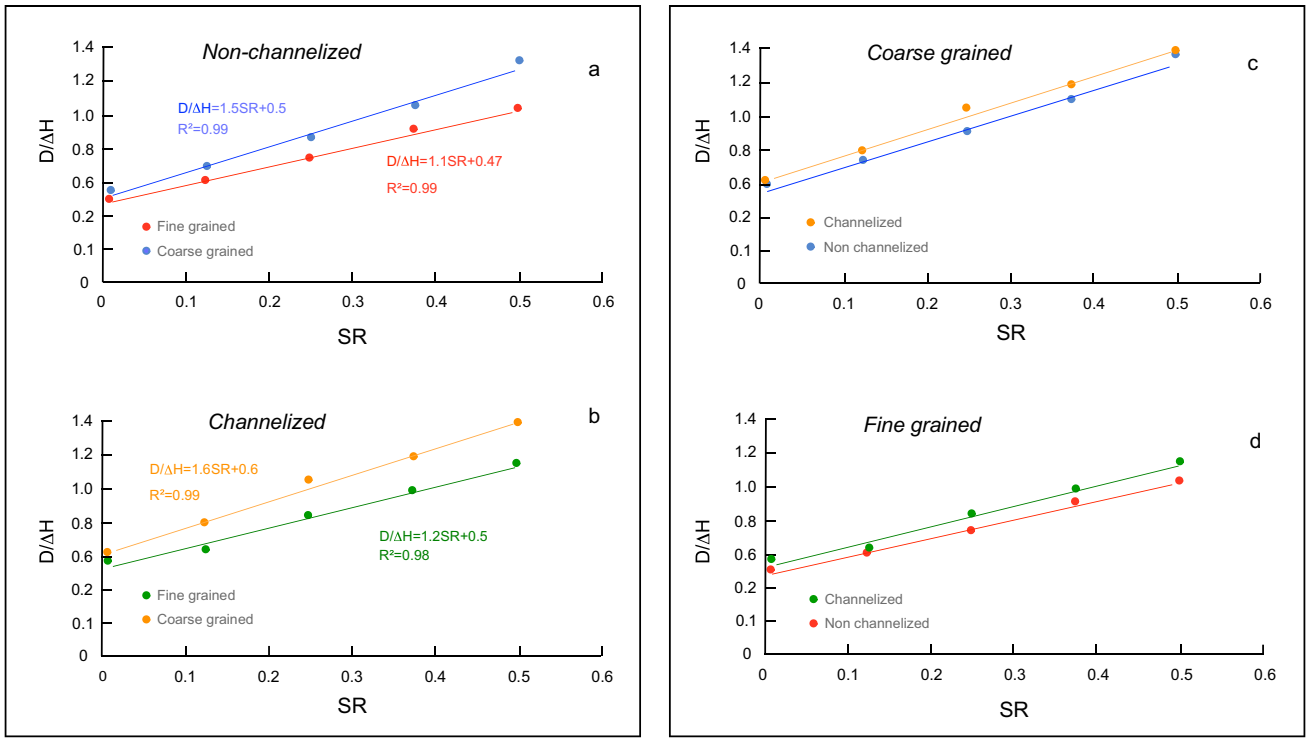

Fig. 3 Diagrams of reverse apparent coefficient of friction (D/ΔH) vs. slope ratio (SR). (**a**) Non-channelized experiments, comparing fine-grained (red) and coarse-grained (blue) experiments. Equation for linear interpolation of data is also reported; (**b**) channelized experiments, comparing fine-grained (green) and coarse-grained (orange) experiments. Equation for linear interpolation of data is also reported; (**c**) comparison of channelized and non-channelized coarse-grained experiments; (**d**) comparison of channelized and non-channelized fine-grained experiments. The equations are the same at equal color

recorded (MT) and ΔH. The MT represents the position of the maximum thickness of the granular material and, due to the geometry of the deposits in channelized and non-channelized experiments, it can be considered as a proxy of the center of mass of the deposits. From Fig. 4a, it is evident how the general behavior described by the normalized maximum thickness vs. SR in non-channelized conditions is similar to that described for the runout, but there is a marked divergence at increasing SRs between coarse-grained and fine-grained material highlighted by different slopes (from 0.55 to 1.05). Under channelized conditions, the relationship between normalized maximum thickness and SR differs significantly. Experiments for both coarse-grained and fine-grained material show almost constant MT/ΔH values (0.08–0.11 for coarse-grained and 0.05 for fine-grained material) at low (coarse-grained flows) and low to intermediate (fine-grained flows) SRs (shaded areas in Fig. 4b). Data at increasing SRs may be linearly fitted (Fig. 4b).

The depositional behavior is also described by means of geometric parameters, such as perimeter (2p) and area (A) of the deposit, measured from images of the (fine-grained) material deposited in the non-channelized experiments (Fig. 2a). In order to generalize these morphometric data and to compare them with those obtained from coarse-grained unconfined experiments (Sulpizio et al. 2016), perimeter and area of the deposit were normalized with respect to ΔH and ΔH^2, respectively. Both areas and perimeters in the different experimental conditions are linearly correlated with SR (Fig. 5a).

Similarly to Sulpizio et al. (2016), we also plotted the flow-front velocity profiles versus the travelled distance for different SRs (Fig. 5b). Velocities of the flows front (v) measured in the expansion box were normalized with respect to the maximum velocity of each experimental run (v_{max}, in the range 5.2–5.5 m/s), the latter measured at the end of the inclined channel. The normalized distance (D) is instead expressed with respect to ΔH. The patterns of the (normalized) velocity vs. (normalized) distance in non-channelized conditions are complex but quite similar between experiments for fine-grained (color lines in Fig. 5b) and coarse-grained flows (grey lines in Fig. 5b), although the normalized values are quite different at equal SRs. The normalized data show a very good fit to a third-order polynomial:

$$\mathrm{v/vmax} = 1 + \mathrm{mD} + \mathrm{nD}^2 + \mathrm{pD}^3 \rightarrow \begin{cases} m = a/\Delta H \\ n = b/\Delta H^2 \\ p = c/\Delta H^3 \end{cases} \quad (1)$$

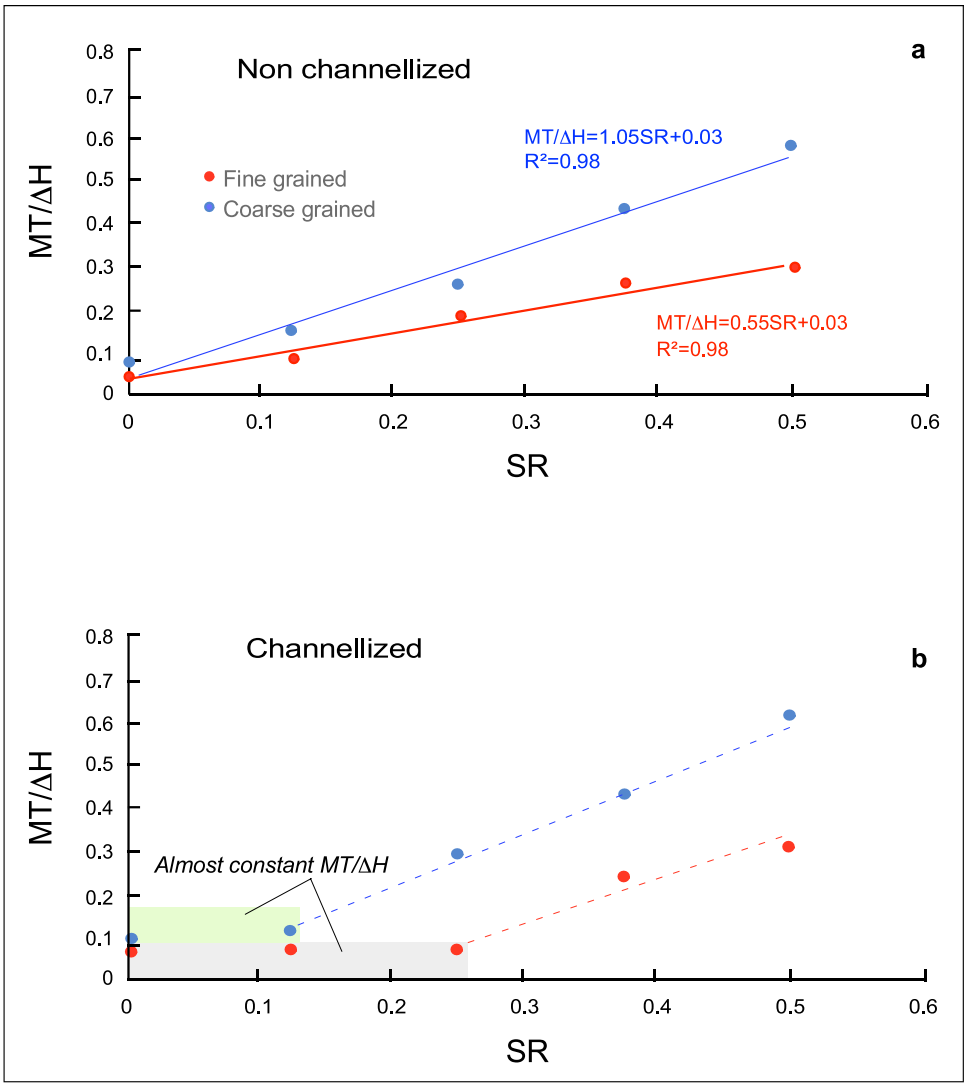

Fig. 4 Diagrams of reverse apparent coefficient of friction of the maximum thickness of the deposits (MT/ΔH) vs. slope ratio (SR). (**a**) Non-channelized experiments, comparing fine-grained (red) and coarse-grained (blue) experiments. Equation for linear interpolation of data is also reported; (**b**) channelized experiments, comparing fine-grained (red) and coarse-grained (blue) experiments. Green and grey-shaded areas indicate the almost constant MT/ΔH values. Equation for linear interpolation of data beyond the constant MT/ΔH values are also reported

with an inflection point defining an intermediate runout region of relatively limited change in velocity (Fig. 5b). As in the case of coarse-grained experiments from Sulpizio et al. (2016), the inflection point coordinates have a positive correlation with SR, and depend on the polynomial coefficients m, n and p, defined as in Fig. 5b. These coefficients are controlled by the variables a, b and c, which depend on the third-order polynomial at changing SR, and can be calculated as functions of SR:

$$\begin{cases} -a = 6.4e^{-2SR} \\ b = 25e^{-3.3SR} \\ -c = 32.2e^{-4.6SR} \end{cases} \quad (2)$$

In order to compare channelized and non-channelized experiments, we also plotted the normalized velocity profiles vs. normalized distance for coarse-grained (Fig. 5c) and fine-grained flows (Fig. 5d). The general behavior of channelized and non-channelized experiments for coarse-grained and fine-grained flows is similar, with only slightly longer runouts of channelized flows with respect to non-channelized ones. It is worth noting that major difference between channelized and non-channelized patterns is observed in the final decelerating paths of the experimental granular flows, and is more evident for SRs greater than 0.125 (Fig. 5c, d). As for the non-channelized experiments of Fig. 5b, the correlation between (normalized) velocity and distance of channelized flows can be expressed as a function of the variables a, b and c:

$$\begin{cases} -a = 3.2e^{-1SR} \\ b = 8.4e^{-1.9SR} \\ -c = 9.2e^{-3.3SR} \end{cases} \quad (3)$$

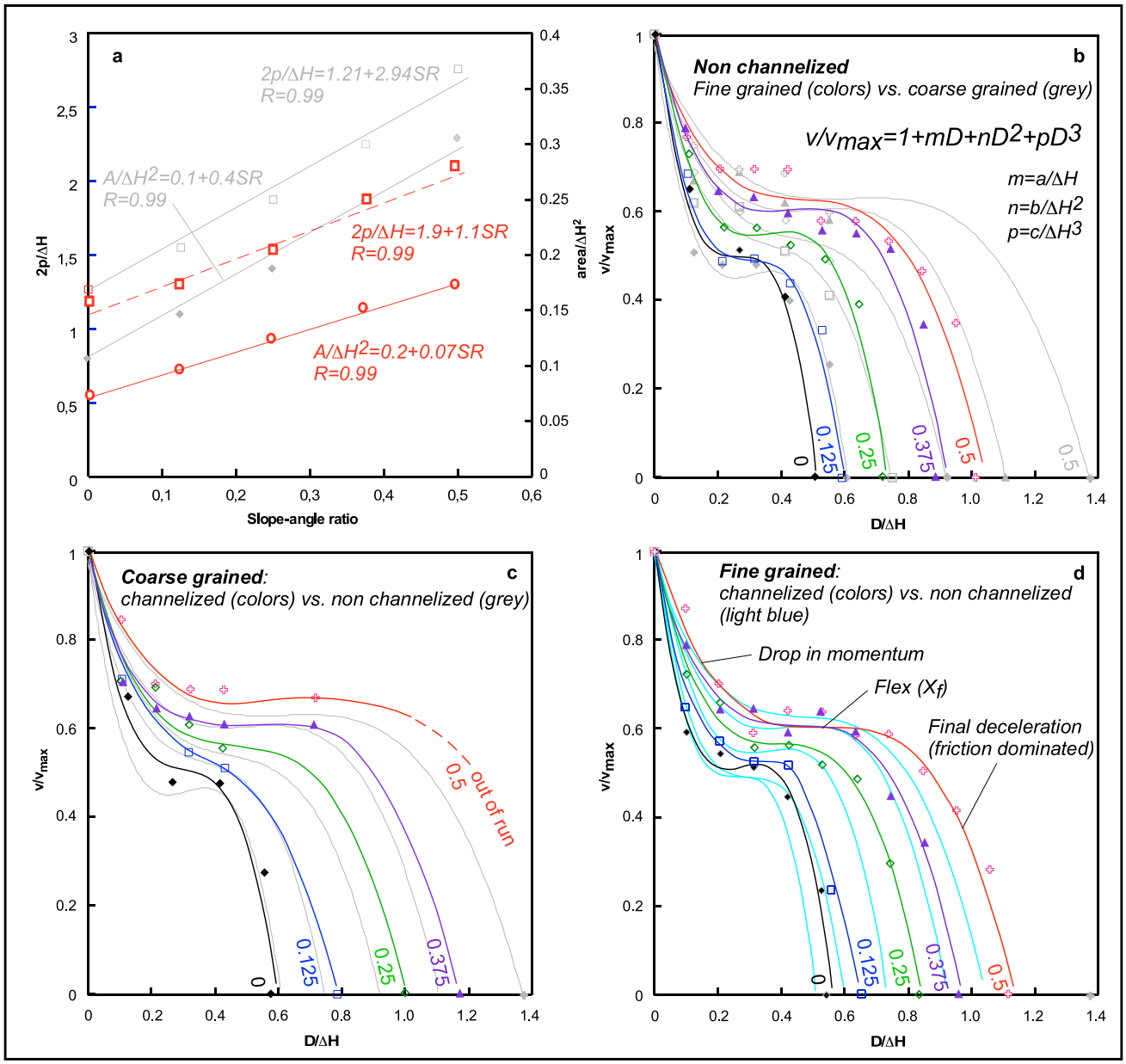

Fig. 5 Diagrams of (**a**) morphometric parameters vs. slope-angle ratio of fine-grained, non-channelized experiments (in red). In grey are reported the morphological data of coarse-grained experiments (from Sulpizio et al. 2016); (**b**) diagram of normalized velocity (velocity/maximum velocity) vs. normalized distance (D/ΔH) for non-channelized experiments. The general form of the third-order polynomial regression is also shown, along with the general expression of parameters m, n and p; (**c**) diagram of normalized velocity vs. normalized distance for coarse-grained experiments; (**d**) diagram of normalized velocity vs. normalized distance for fine-grained experiments. The colored numbers indicate the different slope ratios

for coarse grained flows and:

$$\begin{cases} -a = 4.9e^{-1.6SR} \\ b = 17.8e^{-3SR} \\ -c = 21.5e^{-4.3SR} \end{cases} \quad (4)$$

for fine grained flows.

Discussion

The mobility of granular flows is a major topic in volcanic areas and other sedimentary settings (e.g., Branney and Kokelaar 2002; Lube et al. 2007; Sulpizio et al. 2014). It

is generally expressed as the ratio between the horizontal distance travelled (D) and the height of generation (ΔH), which also helps to define the apparent friction coefficient μD/ΔH (Hayashi and Self 1992). Many factors influence the friction coefficient, and are either internal or external to the granular mixture. Internal factors comprise the grain size distribution (Cagnoli and Romano 2010; 2012), shape of particles and mass (volume) of the material (Rodriguez-Sedano et al. 2016). External factors include channelization (Kokelaar et al. 2014) and the break in slope between the flume and the expansion area, defined here as SR (Sulpizio et al. 2016). The passage over a break in slope is generally claimed as one of the major factors influencing the dynamics of volcanic granular flows (Denlinger and Iverson 2001; Iverson et al. 2004; Zanchetta et al. 2004; Sulpizio and Dellino 2008; Sulpizio et al. 2007; 2008; Sarocchi et al. 2011; Sulpizio et al. 2014). Beyond the break in slope, the reduction in flow velocity induces deposition of material and partial transfer of momentum into the generation of turbulence and elutriation of fines (Gray et al. 2005).

The experiments reported in the present paper for coarse-grained and fine-grained volcanic material in channelized and non-channelized conditions shed light on the effect of grain size and channelization of volcanic granular flows (e.g. concentrated PDCs, volcaniclastic debris flows) moving over a break in slope, as the main (internal and external) factors that control flow dynamics, inundated areas and deposit thickness. Here, different experiment outputs will be discussed in terms of flow runout and inundation area, velocity reduction leading to deposition, and will finally be evaluated for their predictive potential for natural cases.

Runout and inundation areas

Runout and inundation areas are discussed based on the morphometric parameters derived from image analysis of the deposits obtained in the different experimental conditions. Results for coarse-grained, non-channelized flows provided by Sulpizio et al. (2016) are here compared and complemented with those for experimental flows made up of fine-grained material (both channelized and non-channelized) and coarse-grained material in channelized conditions. The elliptical approximation of deposit contours estimated by Sulpizio et al. (2016) also holds for fine-grained deposits in the present experiments (Fig. 2a), which allows for easy extraction of morphometric parameters at changing SRs (Figs. 2a, 5a). In particular, the major axis measured in elliptical deposits coincides with the runout of non-channelized deposits, which were compared with channelized ones (Fig. 3c). It is worth noting that the runout of coarse-grained flows is always greater than that of fine-grained flows. Starting from a common value at SR = 0, the channelized and non-channelized runout diverges at a rate of 0.4 SR (difference between the slopes of the two regression lines in Fig. 3a, b) in coarse-grained flows compared to fine-grained ones (Fig. 3a, b), indicating the strong sensitivity of the reciprocal of the apparent coefficient of friction (μ = D/ΔH) from grain size at increasing SR. This means that curvature radius (defined as the radius of the circle tangent to the two slopes) effects are prevailing at low SR on the dynamics of granular flows, irrespective of their grain size. While the two adopted grain mixtures (coarse and fine-grained) have similar internal and basal friction angles, the divergence of runouts for coarse and fine-grained flows at increasing SR needs to be related to other internal effects than energy dissipation by friction with the substratum.

We cannot advocate a mass dependence of the runout difference (Rodriguez-Sedano et al. 2016) because the mass of the fine and coarse-grained material in the different experiments is the same (Fig. 1b). What is different is only the mass distribution along the vertical profile of the moving flow, which shows clear reverse grading of the larger clasts in the case of coarse-grained experimental flows (Sulpizio et al. 2016). This flow stratification concentrates the maximum of momentum at the top of the moving granular mixture, which is the portion of the flow least influenced by friction. This also explains why the grain size effect becomes more pronounced with increasing SR, as the momentum partitioning of a flow crossing a slope break becomes more effective when transitioning from low to high SR values (Denlinger and Iverson 2001), in accordance with the equation:

$$q_{bs} = (m2\pi r - \frac{mv^2}{r}) \quad (5)$$

where q_{bs} is the momentum breakdown passing over a break in slope of radius r (with increasing r corresponding to higher SR), m is the mass of the granular mixture, $2\pi r$ and v^2/r are the tangential and centripetal accelerations per unit time.

In this respect, there is a limited influence of flow channelization, with confinement effect that impacts on flow runout only for 0.1 SR for both the grain size distributions (Fig. 3c, d). We can consider this slight difference as due to the energy dissipated for the lateral spreading in non-channelized experimental flows.

The dependence of the reciprocal of the apparent coefficient of friction by grain size is even more evident when it is considered relative to the center of mass of the deposit (MT) rather than to the run-out ($\mu_{MT} = MT/\Delta H$) for non-channelized experiments (Fig. 4a). In this case the linear fittings for coarse-grained and fine-grained flows yield a difference in slope of 0.5 SR. The almost constant value of μ_{MT} at low SRs (Fig. 4b) suggests that increased SR

(increasing curvature radius, i.e. smoother transition between channel and depositional area) is less effective than an increased area over which friction applies, represented by the lateral walls of the channel. If we consider the balance between inertial and frictional forces, it is evident how the first are prevalent for SR > 0.125 for coarse grained mixtures, or 0.250 for fine grained ones (Fig. 4b), indicating again how abundance of fine-grained grain sizes, together with particle segregation, increases effectiveness of frictional forces.

Finally, the values of normalized perimeter and area for fine-grained non-channelized flows relative to SR have linear fittings similar to those for the coarse-grained ones (Sulpizio et al. 2016), but they yield lower slopes (Fig. 5a). This indicates a higher internal friction between the (fine) grains, which limited the surface covered by the deposits (corresponding to the inundated area) with respect to the coarse-grained experimental flows.

Velocity decay beyond the break in slope

The deceleration paths of experimental coarse and fine-grained granular flows in channelized and non-channelized conditions show the same trends, independently on SR. The normalized velocity profiles show three distinct phases of deceleration: (i) initial strong deceleration due to sudden drop in the driving force; (ii) almost invariant, inertia-dominated deceleration; (iii) final, friction-dominated rapid deceleration (Fig. 5b). The runout decreases in fine-grained flows with respect to coarse-grained ones at increasing SR, as already discussed in the previous subsection. The same holds when comparing normalized velocity profiles for channelized vs. non-channelized experimental flows. All the profiles show third-order polynomial fits according to the general form:

$$v/v_{max} = 1 + mD + nD^2 + pD^3 \quad (6)$$

where m = a/Δ H, n = b/Δ H^2, p = c/Δ H^3, and a, b, c are the parameters of the third-order polynomial at changing SR (Table 2).

The passage from the initial drop in momentum and the final friction-dominated deceleration tract can be identified in the position of the flex of the third order polynomials (X_f; Fig. 5d). Figure 6 shows how X_f increases with SR, with no significant differences between channelized and non-channelized experimental flows and only a slight difference between coarse- and fine-grained flows.

Implication for natural granular flows

The empirical relationships extracted from laboratory experiments provide useful insights for better understand the dynamics of transportation and deposition of natural granular flows. In particular, experiments demonstrated how, at equal boundary conditions, channelization has not a decisive effect in increasing flow runouts. On the other hand, fine grained mixtures show shorter runouts at increasing SR with respect to coarse grained mixtures (Fig. 3), indicating how grain size distribution is prevalent with respect to topographic control for determining the flow runout.

The experiment outputs seem to contradict some data from natural cases, which suggest higher mobility for fine grained PDCs or volcanoclastic flows (i.e. mud flows). As an example, fine grained PDCs generated from column/fountain collapse during the Montserrat eruption in the period 1995–1998 were reported to have longer runout and inundate

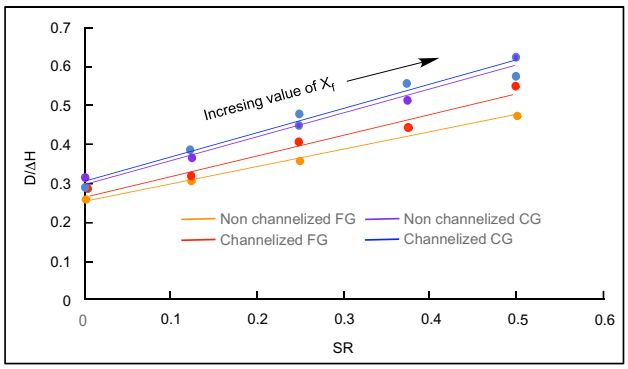

Fig. 6 Diagram showing the position of flex of third-order polynomials of Fig. 5 vs. SR for the different combinations of grain size and channelization and non-channelization

Table 2 Variations of parameters *a*, *b* and *c* of the third-order polynomial fit at changing SR and for the various combination of grain size and channelization

Coarse grained, channelized				Fine grained, channelized			Coarse grained, not channelized			Fine grained, not channelized		
Slope ratio	a	b	c	a	b	c	a	b	c	a	b	c
0	3.3	9.3	11	5.5	20.4	24.3	5.5	18.29	19.57	6	23.5	30.8
0.125	2.7	5.9	5.2	3.7	11	11.7	3.3	8.51	7.8	5.1	14.8	18.5
0.250	2.5	5.1	1.6	3.1	7.5	6.3	2.7	5.8	4.34	4.2	12.1	11.4
0.375	2.3	4.3	2.5	2.5	5.8	4.4	2.2	4.48	2.93	1	7.1	5.6
0.5	1.9	1.4	2	2.4	4.4	2.7	1.72	2.81	1.51	2.2	4.5	1.2

larger areas with respect to coarse grained PDCs from dome collapses (Calder et al. 1999). In volcaniclastic flows, mud flows are considered more mobile than coarse grained debris flows, as in the case of Osceola mud flow from Mount Rainier (USA; Vallance and Scott 1997).

In order to shed light on the effect of fine-grained material on flow dynamics, two experiments were carried out using 2-mm particles as coarse grain size and adding (i) different weight % of 0.25 mm particles (Fig. 7a) and, (ii) 50% in weight of 1 mm, 0.5 mm, 0.25 mm and 0.125 mm particles (Fig. 7b). These experiments resemble those carried out using small scale apparatus (Linares-Guerrero et al. 2007; Phillips et al. 2006). Figure 7 summarizes the experimental results, and highlight the first order, negative linear dependence of runout from abundance of fine particles (Fig. 7a) and from the dimension ratio (d_{ratio}; Fig. 7b). In particular, experimental results provide empirical relationships for runout:

$$\begin{cases} runout = 2.6 - 0.01 fine\% \\ runout = 1.3 - 0.04 d_{ratio} \end{cases} \quad (7)$$

Although not directly scalable to nature, these experiments highlight how the runout is slightly more sensitive to d_{ratio} (decay ratio of 0.04) with respect to *fine%* (decay ratio of 0.01).

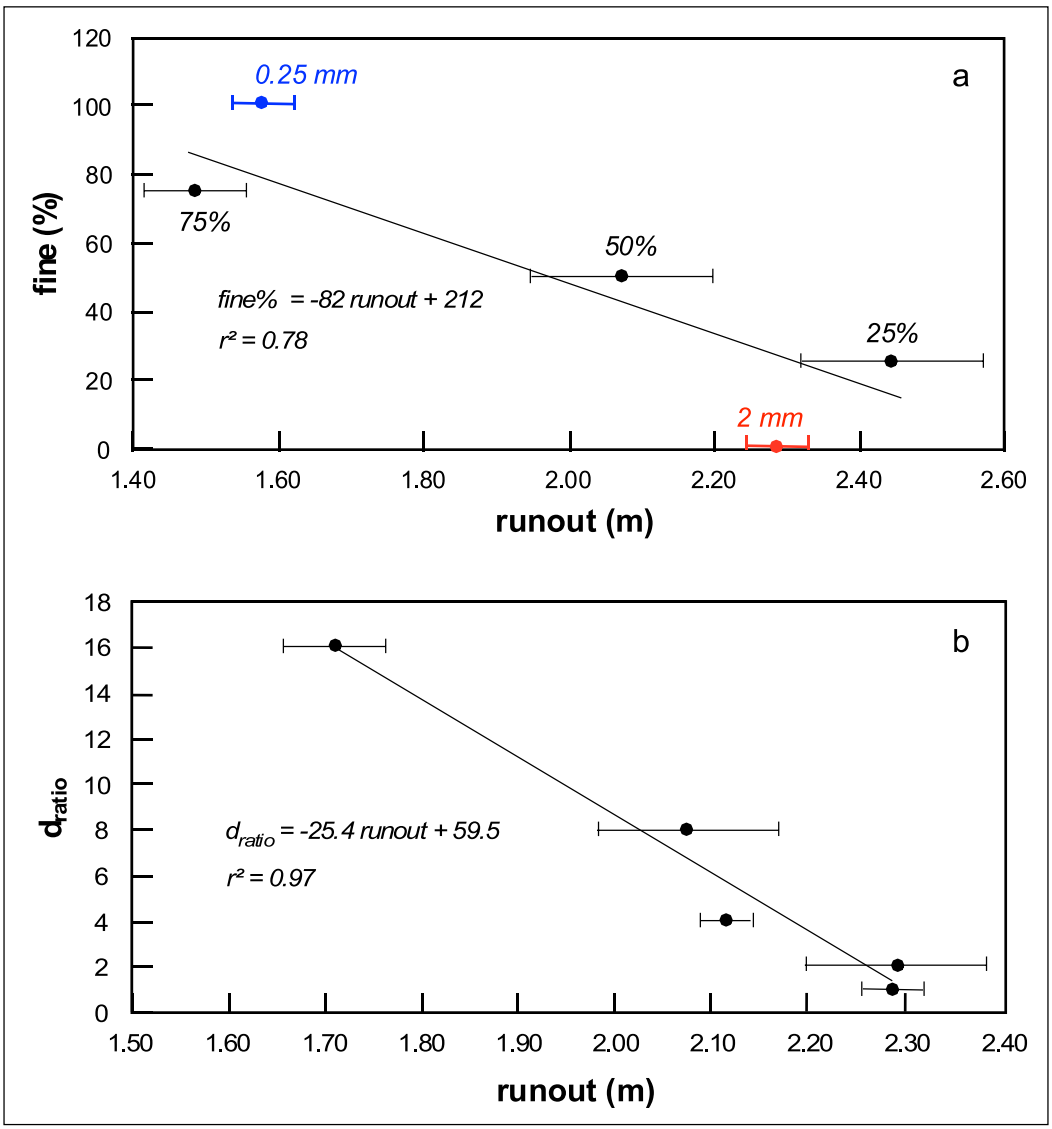

Fig. 7 Diagrams showing the runout dependence on the amount of fine particles in the mixture, using the grain size of 2 mm as coarse grain size class. (**a**) Runout as function of the % of 0.25 mm grain size added to the 2 mm one; (**b**) runout of mixture composed of 50% of 2-mm grain size and 1 mm, 0.5, 0.25 and 0.125 grain size classes. $d_{ratio} = \frac{2mm}{d_{particles}}$

This apparent contradiction between experiments and natural flows may be explained by other mechanisms that in nature may alter the simple relationships found in the experiments. First of all, fine grain size of the solid particles can promote fluid (gas or water) retention within the mixture, promoting fluidization (Druitt et al. 2007; Iverson 1997). Fluidization reduces granular contacts, which are the primary source of energy consumption due to frictional forces. As an example, fluidization was claimed as main mechanism explaining the longer runouts of slow moving, ignimbrite-forming concentrated PDCs (Roche et al. 2016). Efficiency of fluidization depends on many factors, including topographic roughness, amount of gas in eruptive mixture or water in volcaniclastic flow, and type of substratum. In any case, the most prevalent parameter is the permeability of the solid mixture, which controls the rate of fluid escape from the moving flow (Bourgisser 2012; Sulpizio et al. 2014). Permeability is the combination of different physical properties of the moving mixture, including flow expansion, grain size distribution and shape and sorting of solid particles (Bourgisser 2012). Flow expansion depends mainly on granular temperature, which measures the state of agitation of solid particles, and is proportional to the square of flow velocity. The higher the flow expansion, the easier the gas escape. This effect reduces effectiveness and duration of fluidization state in the flow. Grain size distribution controls the rate of fluidization vs. elutriation of very fine-grained particles, which impinge on the retention of fluid within the moving flow. Finally, shape of particles determines the tortuosity of fluid paths, which rules the time of fluid escape from the solid mixture (Bourgisser 2012).

From the parameters discussed above, it is evident how the fluidization strongly depends on availability of fluid sources and characteristics of solid particles. Applying these characteristics to our experiments, it emerges how there are not internal (e.g. magmatic gas from breakage of juvenile clasts, expansion of heated of entrapped air) nor external (e.g. water filled sediments, vegetation) fluid sources to the moving mixture. Also, the air ingestion of air from flow front is not effective, except for the expanded front, as demonstrated by inspection of experiment video-records (Sulpizio et al. 2016).

The coarse grain size distribution of the experimental material shows more than 90% of particles coarser than 0.5 mm and ca. 20% coarser than 2 mm (Fig. 1b), which seems not adequate to retain the (small) amount of gas (air) available within the moving flow. On the other hand, the mixture used for fine grained experiments shows a very good sorting, which increases permeability.

This justifies why our experimental flows largely appear non-fluidized granular flows, and the apparent contradiction of experimental results with some natural cases described in the literature.

All these points suggest that our experimental results are applicable to only natural non-fluidized, fine- to coarse-grained granular flows.

Conclusion

Experimental runs were performed in order to investigate the behavior of coarse-grained and fine-grained volcanic material passing over a break in slope. Channel inclination was maintained fixed at 40°, whereas the inclination of the expansion box was varied between 0° and 20°, at steps of 5°. This experimental setup allowed measuring the flow parameters at different slope-angle ratios (SR) so that lower SRs indicate greater breaks in slope. Experiments were carried out using two grain size distributions of the granular material: coarse grained (30° internal and 35° basal friction angle of material) and fine grained (32° internal and 37° basal friction angle of material).

Experiments results highlight linear dependence of runouts of both coarse-grained and fine-grained mixtures to SR. The slopes of the two regression lines differs of 0.4 SR, indicating the strong sensitivity of the reciprocal of the apparent coefficient of friction ($\mu = D/\Delta H$) on grain size at increasing SR. This means that curvature radius effects are prevailing at low SR on the dynamics of granular flows, irrespective of their grain size. The effect of flow channelization is less effective, with confinement effect that impacts on flow runout only for 0.1 SR for both the grain size distributions.

The deceleration paths of experimental coarse and fine-grained granular flows in channelized and non-channelized conditions show the same trends, independently on SR. The normalized velocity profiles show three distinct phases of deceleration: (i) initial strong deceleration due to sudden drop in the driving force; (ii) almost invariant, inertia-dominated deceleration; iii) final, friction-dominated rapid deceleration.

Finally, caution is recommended for direct application of experimental results to nature, because of the more complex behavior of real fine-rich flows due to possible fluidization effects that can lower energy dissipation within the moving flow.

Acknowledgements We thank the Associated Editor Olivier Roche for the helpful handling of the manuscript, and two anonymous reviewers for the thorough revision of the paper. This study was carried out within the PRIN-PNRR 2022 project P2022CLRTF "Improving the modeling capabilities of geophysical granular flows through experimental and numerical simulations" funded within the European Union Next-GenerationEU (National Recovery and Resilience Plan – NRRP, Mission 4, Component 2, Investment 1.3 – D.D. 1243 2/8/2022, PE0000005). Other funds were also provided by the Fondo de Apoyo a la Investigación of the UASLP projects: C08-FAI-04-11.15 (D. Sarocchi) and CONACyT Ciencia Básica CB 2008-83301-T (D. Sarocchi).

This study was carried out within the RETURN Extended Partnership and received funding from the European Union Next-GenerationEU (National Recovery and Resilience Plan – NRRP, Mission 4, Component 2, Investment 1.3 – D.D. 1243 2/8/2022, PE0000005). RS was supported by the PRIN INSIGHT Project (CP 2022/9MH9AA, CUP: H53D23001490006).

Author contribution Example: RS and DS conceived and designed the research. RS, SM, LARS, OSC and FN conducted experiments. RS, DS, SM, FN, BB and FD analyzed data. RS wrote the manuscript. All authors read and approved the manuscript.

Funding Open access funding provided by Università degli Studi di Bari Aldo Moro within the CRUI-CARE Agreement. PRIN-PNRR 2022 project P2022CLRTF "Improving the modeling capabilities of geophysical granular flows through experimental and numerical simulations" funded within the European Union Next-GenerationEU (National Recovery and Resilience Plan – NRRP, Mission 4, Component 2, Investment 1.3 – D.D. 1243 2/8/2022, PE0000005). PRIN INSIGHT Project (CP 2022/9MH9AA, CUP: H53D23001490006).

Availability of data and materials Experimental results are available under request at the senior author.

Declarations

Ethical approval No humans and/or animals used in this work.

Conflict of interest The authors declare no competing interests.

References

Bernard J, Kelfoun K, Le Pennec J-L, Vallejo Vargas S (2014) Pyroclastic flow erosion and bulking processes: comparing field-based vs. modeling results at Tungurahua volcano, Ecuador. Bull Volcanol 76:858. https://doi.org/10.1007/s00445-014-0858-y

Bourgisser A (2012) A semi-empirical method to calculate the permeability of homogeneously fluidized pyroclastic material. J Volcanol Geotherm Res 243–244:97–106

Branney M, Kokelaar B (2002) Pyroclastic density currents and the sedimentation of ignimbrites. Geol Soc London Mem 27:1–143

Breard ECP, Dufek J, Lube G (2018) Enhanced mobility inconcentrated pyroclastic densitycurrents: an examination of aself-fluidization mechanism. Geophys Res Lett 45:654–664. https://doi.org/10.1002/2017GL075759

Cagnoli B, Romano GP (2010) Effect of grain size on mobility of dry granular flows of angular rock fragments: an experimental determination. J Volcanol Geotherm Res 193:18–24

Cagnoli B, Romano GP (2012) Effects of flow volume and grain size on mobility of dry granular flows of angular rock fragments: a functional relationship of scaling parameters. J Geophys Res. https://doi.org/10.1029/2011JB008926

Calder ES, Cole PD, Dade WD, Druitt TH, Hoblitt RP, Huppert HE, Ritchie L, Sparks RSJ, Young SR (1999) Mobility of pyroclastic flows and surges at the Soufriere Hills Volcano, Montserrat. Geophys Res Lett 26(5):537–540

Calder ES, Sparks RSJ, Gardeweg MC (2000) Erosion, transport and segregation of pumice and lithic clasts in pyroclastic flows inferred from ignimbrite at Lascar Volcano, Chile. J Volcanol Geotherm Res 104:201–235

Campbell CS (2006) Granular material flows—an overview. Powder Technol 162:208–229

Cole PD, Fernandez E, Duarte E, Duncan AM (2005) Explosive activity and generation mechanisms of pyroclastic flows at Arenal volcano, Costa Rica between 1987 and 2001. Bull Volcanol 67:695–716

Dade WB, Huppert HE (1998) Long-runout rockfalls. Geology 26(9):803–806

Denlinger RP, Iverson RM (2001) Flow of variably fluidized granular masses across three-dimensional terrain. Part II. Numerical predictions and experimental tests. J Geophys Res 106:553–566

Druitt TH, Avard G, Bruni G, Lettieri P, Maez F (2007) Gas retention in fine-grained pyroclastic flow materials at high temperatures. Bull Volcanol 69:881–901

Felix G, Thomas N (2004) Relation between dry granular flow regimes and morphology of deposits: formation of levees in pyroclastic deposits. Earth Planet Sci Lett 221:197–213

Gray JMNT, Wieland M, Hutter K (1999) Free surface flow of cohesionless granular avalanches over complex basal topography. Proc R Soc Lond A Math Phys Eng Sci 455:1841–1874

Gray TE, Alexander J, Leeder MR (2005) Quantifying velocity and turbulence structure in depositing sustained turbidity currents across breaks in slope. Sedimentology 4:1–22

Gurioli L, Sulpizio R, Cioni R, Sbrana A, Santacroce R, Luperini W, Andronico D (2010) Pyroclastic flow hazard assessment at Somma-Vesuvius based on the geological record. Bull Volcanol 72:1021–1038. https://doi.org/10.1007/s00445-010-0379-2

Hayashi JN, Self S (1992) A comparison of pyroclastic flow and debris avalanche mobility. J Geophys Res 97:9063–9072

Iverson R (1997) The physics of debris flows. Rev Geophys 35:245–296

Iverson RM (2015) Scaling and design of landslide and debris-flow experiments. Geomorphology 244:9–20. https://doi.org/10.1016/j.geomorph.2015.02.033

Iverson RM, Vallance JW (2001) New views of granular mass flows. Geology 29:115–118

Iverson RM, Logan M, Denlinger RP (2004) Granular avalanches across irregular three-dimensional terrain: 2. Experimental tests. J Geophys Res Earth Surf 109:F01015

Jones TJ, Beckett F, Bernard B, Breard E, Dioguardi F, Dufek J, Engwell S, Eychenne J (2023) Physical properties of pyroclastic density currents: their importance, relevance, challenges, and future directions. Front Earth Sci 11:1218645. https://doi.org/10.3389/feart.2023.1218645

Kokelaar BP, Graham RL, Gray JMNT, Vallance JW (2014) Fine-grained linings of leveed channels facilitate runout of granular flows. Earth Planet Sci Lett 385:172–180

Linares-Guerrero E, Goujon C, Zenit R (2007) Increased mobility of bidisperse granular avalanches. J Fluid Mech 593:475–504. https://doi.org/10.1017/S0022112007008932

Louge M, Turnbull B, Carroll C (2012) Volume growth of a powder snow avalanche. Ann Glaciol 53:57–60

Lube G, Cronin SJ, Platz T, Freundt A, Procter JN, Henderson C, Sheridan MF (2007) Flow and deposition of pyroclastic granular flows: a type example from the 1975 Ngauruhoe eruption, New Zealand. J Volcanol Geotherm Res 161:165–186

Lube G, Huppert HE, Sparks RSJ, Freundt A (2011) Granular column collapse down rough, inclined channels. J Fluid Mech 675:347–368

Macias JL, Espindola JM, Bursik MI, Sheridan MF (1998) Development of lithic-breccias in the 1982 pyroclastic flow deposits of El Chichon volcano, Mexico. J Volcanol Geotherm Res 83:173–196

Mulder T, Alexander J (2001) The physical character of subaqueous sedimentary density flows and their deposits. Sedimentology 48:269–299

Palladino DM, Giordano G (2019) On the mobility of pyroclastic currents in light of deposit thickness and clast size trends. J Volcanol Geotherm Res 384:64–74

Phillips JC, Hogg AJ, Kerswell RR, Thomas NH (2006) Enhanced mobility of granular mixtures of fine and coarse particles. Earth Planet Sci Lett 246:466–480. https://doi.org/10.1016/j.epsl.2006.1004.1007

Pudasaini SP (2012) A general two-phase debris flow model. J Geophys Res 117:F03010

Pudasaini SP, Hutter K (2007) Avalanche dynamics—dynamics of rapid flows of dense granular avalanches. Springer-Verlag, Berlin, p 602. https://doi.org/10.1007/978-3-540-32687-8

Roche O, Buesch DC, Valentine GA (2016) Slow-moving and far-travelled dense pyroclastic flows during the Peach Spring super-eruption. Nat Commun 7:10890. https://doi.org/10.1038/ncomms10890

Rodriguez-Sedano LA, Sarocchi D, Sulpizio R, Borselli L, Campos G, Moreno Chavez G (2016) Influence of particle density on flow behavior and deposit architecture of concentrated pyroclastic density currents over a break in slope: insights from laboratory experiments. J Volcanol Geotherm Res 328:178–186. https://doi.org/10.1016/j.jvolgeores.2016.10.017

Sarocchi D, Sulpizio R, Macías JL, Saucedo R (2011) The 17 july 1999 block-and-ash flow (BAF) at Colima Volcano: new insights on volcanic granular flows from textural analysis. J Volcanol Geotherm Res 204(1–4):40–56

Sulpizio R, Dellino P (2008) Sedimentology, depositional mechanisms and pulsating behaviour of pyroclastic density currents: Caldera volcanism: analysis, modelling and response. In: Gottsman J, Marti J (eds) Developments in Volcanology 10. Elsevier, Amsterdam, pp 58–96

Sulpizio R, Mele D, Dellino P, La Volpe L (2007) Deposits and physical properties of pyroclastic density currents during complex Subplinian eruptions: the AD 472 (Pollena) eruption of Somma-Vesuvius, Italy. Sedimentology 54:607–635

Sulpizio R, De Rosa R, Donato P (2008) The influence of variable topography on the depositional behaviour of pyroclastic density currents: the examples of the Upper Pollara eruption (Salina Island, southern Italy. J Volcanol Geotherm Res 175:367–385

Sulpizio R, Bonasia R, Dellino P, Mele D, Di Vito MA, La Volpe L (2010) The pomici di Avellino eruption of Somma-Vesuvius (3.9 ka BP). Part II: sedimentology and physical volcanology of pyroclastic density current deposits. Bull Volcanol 72:559–577

Sulpizio R, Dellino P, Doronzo DM, Sarocchi D (2014) Pyroclastic density currents: state of the art and perspectives. J Volcanol Geotherm Res 283:36–65

Sulpizio R, Castioni D, Rodriguez-Sedano LA, Sarocchi D, Lucchi F (2016) The influence of slope-angle ratio on the dynamics of granular flows: insights from laboratory experiments. Bull Volcanol 78:77. https://doi.org/10.1007/s00445-016-1069-5

Tanguy JC, Ribiere C, Scarth A, Tjetjep WS (1998) Victims from volcanic eruptions: a revised database. Bull Volcanol 60:137–144

Tilling RI, Lipman PW (1993) Lessons in reducing volcanic risks. Nature 364:77–280

Turnbull B, McElwaine JN, Ancey C (2007) Kulikovskiy–Sveshnikova–Beghin model of powder snow avalanches: development and application. J Geophys Res. https://doi.org/10.1029/2006JF000489

Vallance JW, Scott KM (1997) The osceola mudflow from Mount Rainier: sedimentology and hazard implications of a huge clay-rich debris flow. Geol Soc Am Bull 109(2):143–163

Vallet J, Turnbull B, Joly S, Dufour F (2004) Observations on powder snow avalanches using videogrammetry. Cold Reg Sci Technol 39(2–3):153–159. https://doi.org/10.1016/j.coldregions.2004.05.00

Zanchetta G, Sulpizio R, Pareschi M, Leoni F, Santacroce R (2004) Characteristics of May 5–6, 1998 volcaniclastic debris flows in the Sarno area (Campania, southern Italy): relationships to structural damage and hazard zonation. J Volcanol Geotherm Res 133:377–393